Solubility, mutual diffusivity, specific volume and interfacial tension of molten PCL/CO₂ solutions by a fully experimental procedure: effect of pressure and temperature

Maria Giovanna Pastore Carbone [a], Ernesto Di Maio [a,*], Giuseppe Scherillo [a], Giuseppe Mensitieri [a], Salvatore Iannace [b]

[a] Department of Materials and Production Engineering, Faculty of Engineering, University of Naples Federico II, P.le Tecchio 80, 80125 Naples, Italy
[b] Institute for Composite and Biomedical Materials, National Research Council, P.le Tecchio 80, 80125 Naples, Italy

ABSTRACT

Solubility, diffusivity, specific volume and interfacial tension of molten poly(ε-caprolactone)/CO₂ solutions have been simultaneously measured by using a fully experimental technique. This technique, based on the coupling of a gravimetric measurement with the Axisymmetric Drop Shape Analysis (ADSA), provides all of the aforementioned properties in a single experiment, without relying on any theoretical assumption or equation of state at any stage of the properties evaluation. Measurements have been performed at three different temperatures (80, 90 and 100 °C) and at CO₂ pressures up to 4.2 MPa. Dependencies of the aforementioned properties upon temperature and CO₂ pressure have been highlighted. Sorption isotherms have been modeled using the Sanchez–Lacombe lattice theory, while the interfacial tension data have been interpreted by using empirical correlations.

© 2012 Elsevier B.V. All rights reserved.

1. Introduction

Use of supercritical fluid in processing of polymeric materials has been widely investigated and adopted, in the last decades, for the manufacture of several types of products, such as foams, microparticles, membranes and fibers [1,2]. In particular, gas foaming technologies have been drawing increased attention because of the extremely wide range of application of polymeric foams in fields such as packaging, acoustic and thermal insulation, tissue engineering and separation processes [3]. The development of supercritical fluid foaming techniques, for example, paved the way to the production of microcellular foams, in which mean pore diameter is smaller than 10 μm and population density is larger than 10⁹ cells per cm³ and which are characterized by improved mechanical and impact properties as compared to standard foams [4]. In fact, fine tuning of processing conditions and selection of blowing agent allows the tailoring of the structure of a foam and, in turn, its final properties, to the specific application [5–7]. In this context, modeling of the foaming process represents a challenging

issue in order to develop effective design tools allowing the prediction of foam structure on the basis of process conditions. To this aim, availability of theoretical as well as empirical correlations among process variables, foam structure and final properties is of paramount importance.

Recent efforts in modeling of foam formation have addressed simultaneous nucleation and growth phenomena as inspired by the pioneering work of Shafi and Flumerfelt [8] and of Taki [9]. In particular, bubble nucleation is commonly dealt with by referring to classical theory of homogeneous nucleation, derived, in its original form, for droplet formation from the vapor phase [10]. Developments of this theory to account for bubble formation in polymer/gas solutions were proposed, among others, by Colton and Suh [11], Goel and Beckman [12], Baldwin et al. [4] and Han and Han [13], which provided a semi-quantitative frame for the investigation of the effect of working conditions (e.g. temperature and gas pressure) and thermodynamic, interfacial and mass transport properties of polymer/gas solutions on the kinetics of foam formation and on pore structure of the foam. In particular, those properties which play a role in the homogeneous bubble nucleation in thermoplastic polymers induced by dissolved gas are: gas solubility, low molecular weight compound/polymer mutual diffusivity, interfacial tension and specific volume of the polymer/gas

---

* Corresponding author. Tel.: +39 081 768 25 11; fax: +39 081 768 24 04.
 E-mail address: edimaio@unina.it (E. Di Maio).

solution. In addition to the aforementioned properties, the rheological behavior of polymer/gas solutions plays an important role in the control of the growth stage [14–17], until the vitrification or crystallization of the polymeric matrix lock-in the foamed structure [18,19]. Bubble growth is governed by heat, mass and momentum balances and the approaches proposed in the literature are fully quantitative, provided that the constitutive equations for the rheological, interfacial, mass transport and thermal properties are available. Therefore, from the previous discussion, it is clear that the knowledge of the involved phenomena and the availability of information on the aforementioned properties are important to utilize the cited simultaneous nucleation and growth models of foam formation. It is worth of note, here, that the properties of interest in these models are the non-equilibrium ones, in correspondence to the gas/polymer interphase, since characteristic time of the involved phenomena are much shorter that those required to attain local equilibrium. Furthermore, the macroscopic surface tension may not be quite an adequate descriptor of surface properties for the case of small clusters preceding the bubble (see, for instance, Lee and Flumerfelt in [20]). However, knowledge of equilibrium macroscopic information on polymer/gas solutions may still be useful to those involved in foam modeling, also in view of the difficulties in retrieving more specific information at a molecular level.

In fact, numerous pieces of scientific literature deal with the measurement and modeling/prediction of these properties, the latter being of relevant interest since it is not always easy to perform experiments in the temperature and pressure ranges of interest in the foaming process. Typically, sorption thermodynamics and mass transport properties – e.g. solubility and diffusivity – are determined by means of gravimetric techniques, which consist in continuously weighing the polymer exposed to a gaseous atmosphere. Interfacial tension of the separation surface between a molten polymer–gas solution and gas itself is commonly determined by means of *Axisymmetric Drop Shape Analysis* technique (ADSA), which is based on the evaluation of the shape of an axisymmetric pendant drop [21] and on fitting the shape of the drop to the theoretical drop profile according to the Laplace equation [22,23], properly modified to account for the action of the gravitational field [24–26]. In both of these techniques (i.e. gravimetric and ADSA), the knowledge of the specific volume of molten polymer/gas solution is necessary for the elaboration of the collected data. In fact, regarding the experimental evaluation of solubility in polymers of gases at relatively high pressures, data on specific volume of the polymer/gas solutions are needed in order to correct sorption data from buoyancy effects [27]. When the polymer (either in the glassy [28,29] or in the rubbery [30] state) is exposed to a gaseous penetrant, its volume changes as a consequence of sorption of gas and the compressive action of pressure, thus modifying the buoyancy effect due to gravity. An incorrect evaluation of this effect in turn leads, unavoidably, to an inaccurate evaluation of the sorption data. A possible way to circumvent this difficulty is a trial and error analysis of experimental data performed by combining the gravimetric measurements with the theoretical prediction of the equilibrium mixture density obtained from solution theories grounded on statistical thermodynamics (e.g. Sanchez and Lacombe [31–33] or Simha and Somcynsky [34] equations of state, to mention a few). However, the scarcity of experimental swelling data and, consequently, the actual validation of the effectiveness of the adopted models in correctly predicting the volume of the specific mixture under analysis do suggest a certain caution in using these procedures [35]. As a consequence, a reliable evaluation of the amount of absorbed gas can only be obtained if a direct experimental evaluation of the specific volume of the molten polymer/gas mixture is available.

Regarding the ADSA-based interfacial tension measurement, the interfacial tension of polymer/gas solutions can be measured provided that the coordinates of several points of the drop profile, the specific volume of the fluid surrounding it and the specific volume of the gas saturated polymer drop are available [24–26]. Hence, also in this case, the specific volume of the polymer–gas solution is required for proper calculation.

From this brief description, it is clear how a reliable evaluation of solubility and interfacial tension would certainly benefit from a concurrent volume and weight evaluation in a single experiment under identical experimental conditions. In turn, as stated before, a successful modeling of foaming process relies upon reliable values of these properties. For instance, since nucleation rate is a strong function of interfacial tension (it is, in fact, proportional to $\exp(-\gamma^3)$, according to the classical approach), an inaccurate measurement of this property can lead to a large error in the predictions.

A number of contributions dealt with the precise measurement of sorption as well as interfacial properties of polymer/gas solutions and addressed the need for specific volume evaluation to properly correct the experimental data for the effect of buoyancy. Among others, it is worth to recall here the pioneering works by Jaeger et al., Dimitrov et al. and Park et al. for the details of the proposed approaches [36–38].

In a previous paper, we have presented a purely experimental approach allowing the direct and concurrent determination of solubility, diffusivity, interfacial tension and specific volume of polymer/gas solutions without relying on any theoretical assumption or equation of state at any stage of the properties evaluation [39]. In fact, the adopted approach is based on the coupling of gravimetric gas sorption and ADSA measurements, as already described by Jaeger et al. [36], allowing for the simultaneous measure of those properties in a single experiment. The experimental set-up consists of a magnetic suspension balance equipped with a high pressure and temperature view cell where both gravimetric and interfacial tension measurements are performed at the same time. The pendant drop method (a molten polymer drop hanging from a rod) has been coupled with the classical gravimetric measurement performed on samples placed in a cylindrical crucible. In this experimental configuration, while the magnetic suspension balance is measuring the weight change during sorption of the sample placed in the crucible, the profile of the pendant drop, at the same temperature and pressure, is monitored with a high-resolution camera.

In the present contribution we illustrate the results of our investigation performed with this methodology on molten PCL/CO$_2$ solutions. The choice of this binary system is strongly connected to the recent increasing interest in "eco-friendly" foaming processes, that involve two environmental issues: a biodegradable polymer matrix, that is frequently used to manufacture scaffolds for tissue engineering and that also represents a potential valid alternative to common polymer materials for packaging applications and the use of supercritical carbon dioxide as a blowing agent, that is an alternative to the traditional blowing agents belonging to the class of chlorofluorocarbons, that are known to contribute to seriously deplete the ozone layer [1,5].

In this work, simultaneous measurements of solubility, diffusivity, interfacial tension and specific volume of PCL/CO$_2$ solutions have been performed at three different temperatures (80, 90 and 100 °C) and at CO$_2$ pressures up to 4.2 MPa. Sorption isotherms have been modeled in the light of the Sanchez–Lacombe lattice theory, while the relationships between interfacial tension, the specific volume of the solution and gas concentration have been described by using empirical correlations.

2. Experimental

2.1. Experimental set-up

The experiments were carried out by using a custom-designed measuring device, consisting of a rod to which the polymer–gas solution drop is stuck (for ADSA) and a crucible containing a few grams of polymer–gas solution (for weight monitoring), placed in a high temperature/high pressure (HT–HP) view cell of a magnetic suspension balance (Rubotherm Prazisionsmesstechnik GmbH, Germany). Maximum operating conditions of the equipment are 250 °C and 13.5 MPa. The crucible hangs from the hook of the balance weight measuring unit and the rod is fixed inside the cell in such a way as to avoid any interference with the gravimetric measurement and to allow the reliable continuous acquisition of the drop shape (see Fig. 1). Drop monitoring is made possible through two optical quality windows, mounted perpendicular to the axis of the cell, by using an adjustable high resolution CCD camera (BV-7105H, Appro), equipped with a modular zoom lens system (Zoom 6000, Navitar). A uniform bright background is provided by light
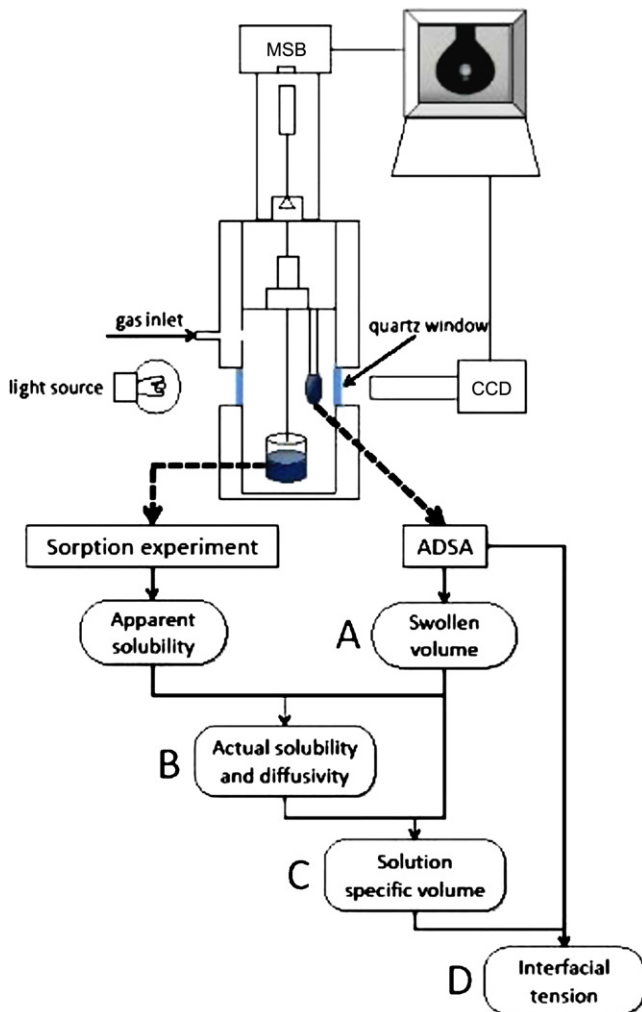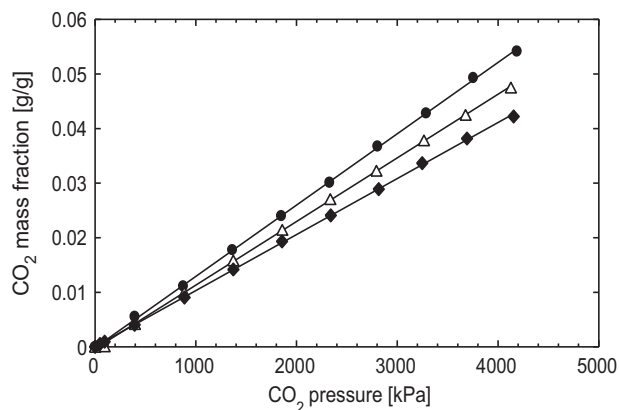

Fig. 1. Schematic illustration of experimental equipment and of data flow used in the coupled sorption–ADSA measurement. Data from ADSA are used to evaluate the volume of the polymer/gas solution contained in the crucible (A), allowing for the correction of sorption data with the proper buoyancy force and, consequently, for the calculation of actual solubility and diffusivity of the polymer/gas solution at each gas pressure (B). From gas sorption amount and solution volume per unit mass of polymer, the specific volume of the polymer/gas solution is then calculated (C). As a final step, this value is fed to the ADSA software to calculate the interfacial tension (D).

emitting diodes, allowing the achievement of an optimal threshold for digitizing the drop image. The CCD camera is connected to a computer, and commercial software (FTA32 Video 2.0, First Ten Angstroms) is used to analyze drop profile.

Full details of the equipment and the description of the preliminary experimental phases, such as drop preparation, optimization of CCD parameters and image calibration (pixel/μm calibration and aberration correction), are given in a previous work [39]. In this measurement, a titanium rod with a diameter of 1.786 mm was chosen as drop holder. The drop was created on the polished bottom surface of the rod by melting ca. 9 mg of neat polymer.

After having placed both the crucible containing the polymer and the rod with the drop in the HT–HP view cell, sorption and ADSA experiments were carried out by isothermal pressure increments up to 4.2 MPa, at 80 °C, and then at 90 and 100 °C. In detail, sorption measurements were conducted by performing step-wise increments of the gas pressure (about 0.5 MPa steps) with pre-heated gas, after the attainment of equilibrium sorption in the previous step. Concurrently, during each pressure step, image acquisition of the pendant drop was performed every 10 min and drop volume was calculated by using the commercial software.

2.2. Materials

Poly(ε-caprolactone), a biodegradable polymer with a melting point of ca. 60 °C, was supplied by Solvay Interox Ltd. (PCL CAPA 6800, Mn = 69,000 ± 1500, Mw = 120,000 ± 2000) and used as received. High purity grade carbon dioxide was supplied by SOL (Italy).

2.3. Data treatment

Data treatment is described in the following according to the measurement flow chart reported in Fig. 1. Details of the whole data treatment chain are described in a previous work [39].

A. *Evaluation of the volume of polymer/gas solution.* For each pressure step, drop volume was estimated from drop profile integration, as performed by the ADSA software. The volume of the polymer/gas solution contained in the crucible, V_c, at equilibrium, can then be calculated as:

$$V_c(T, p) = V_d(T, p)\frac{W_c^0}{W_d^0}, \tag{1}$$

where V_d is the volume of the drop, W_d^0 and W_c^0 are, respectively, the initial weight of the polymer forming the drop and of the polymer contained in the crucible as measured by an analytical balance with a sensitivity of 10^{-5} g (Mettler AE240). It was assumed that, at equilibrium, drop curvature has negligible effects on specific volume and local gas concentration [40] and, consequently, that the drop and the sample in the crucible reach the same volume per unit mass of starting polymer.

B. *Actual solubility and diffusivity.* Data from section A were used for a proper correction of sorption data, to obtain the actual gas weight fraction in the gas/polymer solution (ω_{ACT}), as by Eq. (2).

$$\omega_{ACT}(T, p) = \frac{W_{ACT}^{gas}(T, p)}{W_c^0 + W_{ACT}^{gas}(T, p)} \tag{2}$$

where the actual gas weight gain, W_{ACT}^{gas} is calculated as by Eq. (3):

$$W_{ACT}^{gas}(T, p) = BR_e - BR_e^0 + \rho_{gas}(T, p)[V_c(T, p) + V_h(T)] \tag{3}$$

Here, BR_e is the Rubotherm balance reading at equilibrium at each pressure (polymer/gas solution), BR_e^0 is the initial balance

Fig. 2. Actual sorption isotherms for the PCL/CO$_2$ systems. Experimental data and isotherms predicted by SL-EoS (continuous lines); 80 °C (●); 90 °C (△); 100 °C (◆).

Fig. 3. Comparison between fully experimental sorption isotherm (full circles) and SL-EoS corrected sorption isotherm (open circles). Data refer to 90 °C.

reading at equilibrium (under vacuum), ρ_{gas} is the CO$_2$ density [30], V_h is the volume of crucible and of hook.

The average mutual diffusivity ($\bar{D}$) in each step-wise sorption experiment was calculated as follows [41]:

$$\bar{D} = \frac{\pi L^2}{4} \left(\frac{d(BR_t/BR_\infty)}{d(\sqrt{t})} \right)^2 \tag{4}$$

where BR_t is the balance reading at time at time t, BR_∞ is the balance reading at equilibrium and L is the actual sample thickness (sample is exposed to the gas phase on one side only). The value of $\bar{D}$ calculated through Eq. (4) corresponds to the value of the carbon dioxide mutual diffusivity, $D(C)$ at an intermediate concentration, C, the value of which can be calculated according to the procedures proposed by Vrentas and Duda [42].

C. *Evaluation of specific volume of the solution.* Data from sections A and B allowed for the calculation of the specific volume of the polymer/gas solution, v_s, as by Eq. (5).

$$v_s(T, p) = \frac{V_c(T, p)}{W_c(T, p)} = \frac{V_c(T, p)}{W_c^0 \left(1 + \frac{1}{1 - \omega_{ACT}(T, p)} \right)}, \tag{5}$$

where W_c is the weight of the sample contained in the crucible.
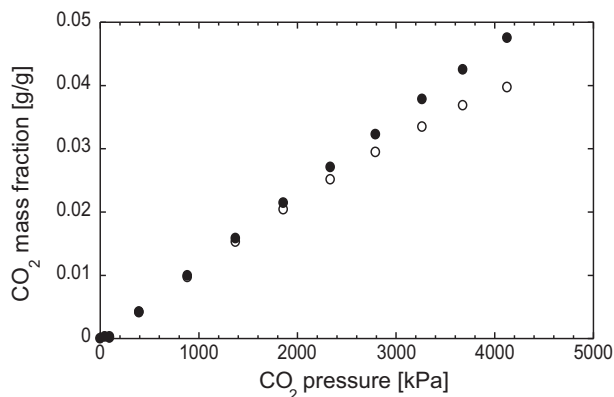D. *Evaluation of interfacial tension of the polymer/gas solution.*

Using the specific volume determined as illustrated in section C, the equilibrium value of interfacial tension was calculated at each value of CO$_2$ pressure by using the ADSA software and, in particular, the algorithm based on the Bashforth–Adams equation (see Refs. [24–26] for details).

3. Results and discussion

3.1. CO$_2$ sorption isotherm in molten PCL

The actual sorption isotherms of CO$_2$ in PCL at the three investigated temperatures are reported in Fig. 2. As expected, ω_{ACT} increases with the pressure and decreases with the temperature.

The experimental data were fitted with the Sanchez–Lacombe equation of state (SL-EoS) for molten polymer/penetrant mixtures [33]. The SL-EoS is a classical compressible lattice fluid theory which has been originally introduced for neat polymers [43] and which has been then extended to the case of polymer/penetrant mixtures by adopting appropriate mixing rules for the reducing parameters of the single components. We refer to the cited literature and references therein for the model description and associated governing equations. Assumption of geometric mean combination rule between the penetrant and the polymer for the characteristic pressure of the mixture allows for a predictive use

of the model in calculating the solubility of the penetrant at specific temperature and pressure conditions. In such a case, the value of the so-called interaction parameter, ψ, is taken as being equal to 1. However, in some cases the interaction parameter is taken as a fitting parameter of experimental solubility data. In fact its value is likely to be different from 1 in the case of mixture components characterized by different types of interaction energies. In the present study, in view of the polar nature of CO$_2$, we used ψ as a fitting parameter and the resulting best-fitting theoretical sorption isotherms are reported in Fig. 2 (continuous lines), along with the solubility data, showing a good fitting capability of the model. Best fitting value determined for ψ is equal to 0.976 ± 0.001 in the whole pressure and temperature range. We utilized for neat PCL the SL-EoS parameters obtained experimentally in a previous work from our group [44] and for CO$_2$ the SL-EOS parameters as taken from the literature [45] (see Table 1).
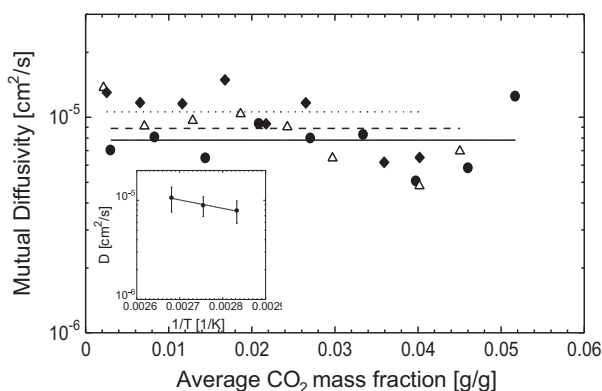
In order to evidence the need for proper buoyancy correction in calculating sorption data, it is useful to compare results gathered from the present fully experimental approach (which allows for a direct measure of volumetric properties of polymer/gas solutions) with other consolidated semi-empirical approaches that adopt a buoyancy correction based upon a theoretical EoS, as proposed, among others, by Li et al. [35]. Accordingly, an iterative algorithm evaluating, by means of the SL-EoS, the fitting parameter ψ and the corresponding specific volume of the polymer–gas solution at each experimental temperature, pressures and calculated gas concentration has been implemented. Convergence of iteration procedure provided the value of ψ by minimizing the difference between the theoretical sorption isotherm predicted by SL model with the experimental sorption isotherm corrected according to the resulting calculated specific volume of the polymer/gas solution. The comparison between the fully experimental sorption isotherm and the semi-empirical, SL-EoS-corrected one is shown in Fig. 3, highlighting a noticeable difference between the two isotherms for gas pressures higher than 2000 kPa (only data at 90 °C are depicted, for the sake of clarity). This finding indicates that the buoyancy correction is an increasingly dominating factor in evaluating gas solubility and that an incorrect evaluation of the specific volume of the polymer–gas solution can lead to relevant errors in the measured property.

3.2. Evaluation of CO$_2$ mutual diffusivity

The values of $\bar{D}$ for carbon dioxide in PCL, as obtained from Eq. (4), are reported in Fig. 4, as a function of CO$_2$ mass fraction. Within the investigated pressure range, it was found that $\bar{D}$ exhibits no significant dependence on CO$_2$ concentration. As expected, we

Table 1
Characteristic SL-EoS parameters of PCL and CO_2 utilized in this study.

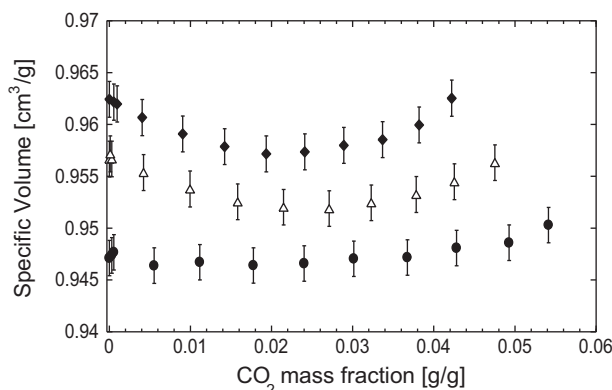|	Characteristic temperatures [K]	Characteristic densities [g/cm^3]	Characteristic pressure [MPa]	Reference
PCL	637.7	1.158	548.6	[44]
CO_2	305.3	1.510	574.5	[45]

Fig. 4. Mutual diffusivity for the PCL/CO_2 solution as a function of CO_2 concentration; 80 °C (●); 90 °C (△); 100 °C (◆). Inset: temperature dependence of average CO_2 mutual diffusivity.

observed an increase of $\bar{D}$ with temperature, with an Arrhenius-type dependence (see the inset in Fig. 4).

3.3. Specific volume of PCL/CO_2 solutions

The specific volume of the PCL/CO_2 solutions is reported in Fig. 5 as a function of CO_2 mass fraction, evidencing a non-monotonic dependence in the experimental pressure and temperature range. This behavior can be justified by observing the dependences of the volume and mass of the drop with CO_2 mass fraction, showed in Fig. 6, where reduced quantities are reported. Clearly, despite the monotonic increase of both drop volume and mass, their ratio (i.e., the specific volume) may follow a non-monotonic dependence on carbon dioxide mass fraction. In fact, when a molten polymer is exposed to a high-pressure gas, two mechanisms compete in affecting the specific volume: (i) compression of the gas saturated polymer melt by the mechanical action of pressure exerted by the external gas; (ii) gas-solubilization. With the increase of external gas pressure, the latter mechanism is responsible for an increase of the volume, while the first is responsible for a reduction of the volume. In our case, the drop volume is monotonically increasing
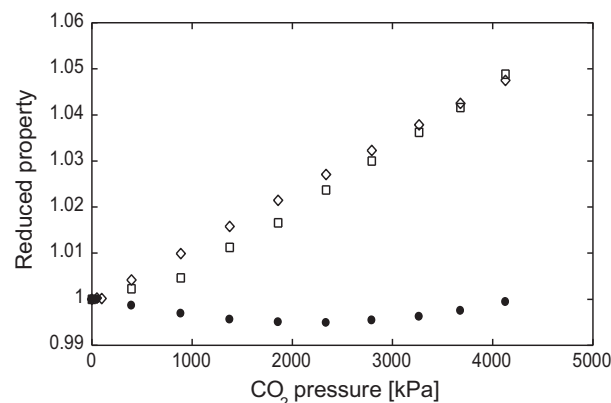
with gas pressure, proving a prevailing effect of the gas solubilization. However, mass increase of the gas saturated polymer drop is occurring. As a final balance, at low gas concentration, the mass increase is the dominant effect, and a reduction of the specific volume is observed. At higher gas concentration, conversely, the volume increase becomes the predominant effect.

There is evidence that carbon dioxide in PCL is present in at least two 'populations' [46]: one 'polymer-associated', i.e. interacting with the PCL carbonyl groups and the other 'nonassociated'. A lower volume of mixing is likely related to polymer-associated species, in view of the interaction that keeps the CO_2 molecules closer to polymer backbone as compared to nonassociated species. It is hence possible that the volume of mixing of polymer with associated CO_2 species is negative, with a total volume of the mixture that is lower than the one calculated on the basis of simple volume additivity. Now, since it is expected that at low pressures (and hence at low concentration of CO_2 inside the polymer) the associated species prevail, on this basis one can justify the experimental finding that at low pressures the specific volume decreases with pressure.
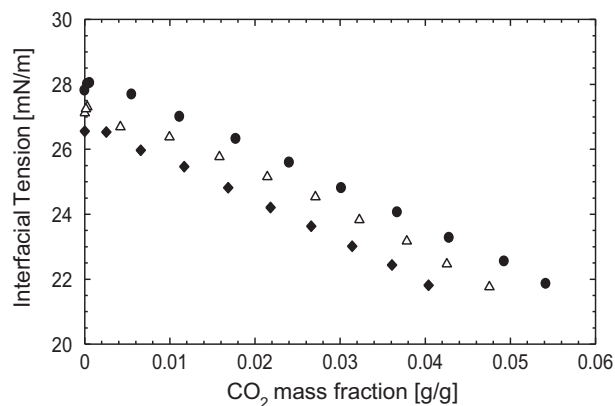
3.4. Interfacial tension

The values of the interfacial tension of the polymer/gas solution, as evaluated on the basis of the procedure described above, are shown in Fig. 7 as a function of CO_2 concentration. In the selected experimental range, interfacial tension of the solution was a nearly linear decreasing function of the CO_2 pressure.

The decrease in the interfacial tension with the gas pressure has already been reported elsewhere [46–50] and is generally attributed to two concurrent phenomena [49,50]: (i) as pressure increases, the free energy density of CO_2 becomes closer to that of the polymer phase and the interfacial tension decreases; (ii) as gas pressure increases, the concentration of CO_2 in the polymer phase increases thus further promoting a decrease of interfacial tension since the two phases in contact become more similar. Temperature drives the interfacial tension down, too: Fig. 8a shows the dependence of the interfacial tension on temperature for the pure polymer and for the polymer–CO_2 solution at about 0.036 mass fraction of gas. It was also estimated that, for the neat PCL,

Fig. 5. Specific volume of the solution PCL/CO_2 as a function of CO_2 mass fraction. Error bars were evaluated by accounting for the whole measurement chain; 80 °C (●); 90 °C (△); 100 °C (◆).
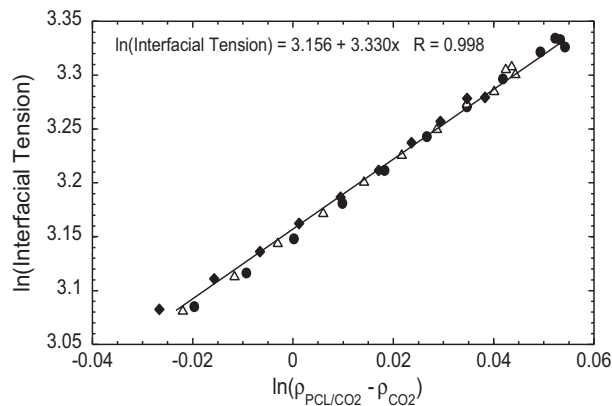

Fig. 6. Volume of the drop, mass and specific volume of the solution, normalized to the initial values, as a function of gas pressure; drop mass (◇), drop volume (□), specific volume of polymer–gas solution (●). Data refer to 90 °C.

Fig. 7. Effect of CO_2 concentration on the interfacial tension of PCL-CO_2 solutions; 80 °C (●); 90 °C (△); 100 °C (♦).

Fig. 9. Macleod plot for the solution PCL/CO_2 in the investigated temperature range; 80 °C (●); 90 °C (△); 100 °C (♦).

the interfacial tension decreases with a temperature coefficient of -0.063 mNm/°C as compared to -0.081 mNm/°C found for the mixture. The dependence of the interfacial tension on gas pressure is shown in Fig. 8b: as observed in the case of polystyrene/CO_2 solutions [47], when reporting the interfacial tension as a function of gas pressure, the data at different temperatures tend to converge at high pressures. This convergence can be ascribed to the counteracting effects of temperature (that, as stated before, leads to the reduction of the interfacial tension) and of solubility of CO_2 in the polymer, that decreases with temperature and results into a higher value of interfacial tension.

A common and widely used treatment of interfacial tension data, known as the parachor method, is based on the collapse of interfacial tension data on a master curve when reported as function of
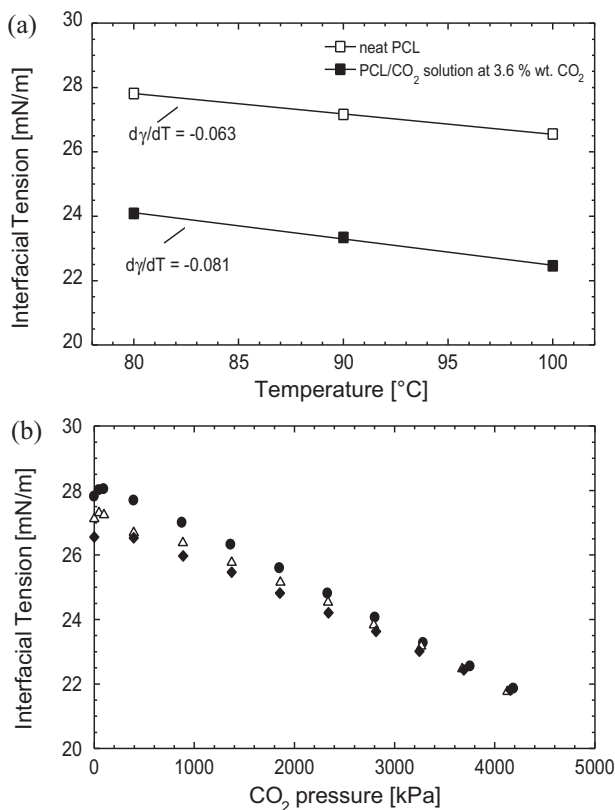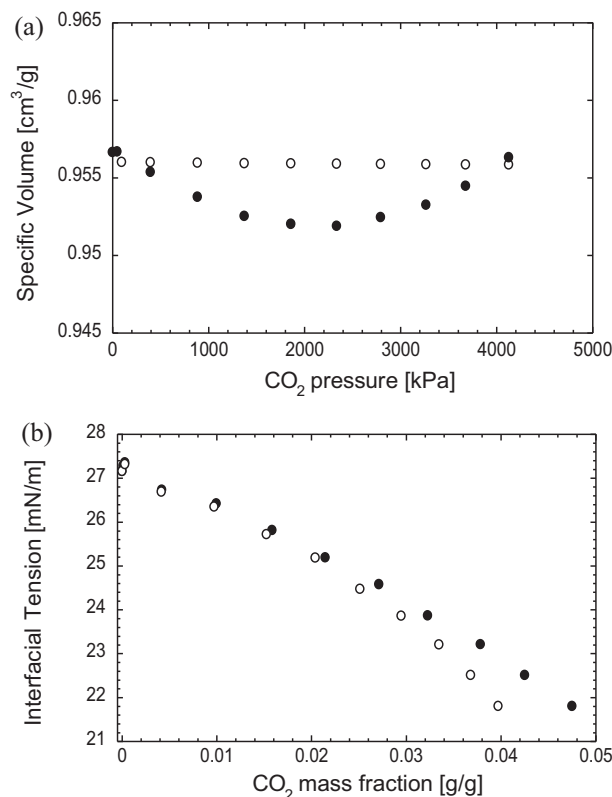
the difference of densities between the gas and the liquid phase (in our case the molten polymer/gas solution). Macleod proposed the following expression:

$$\gamma_{sol} = P(\rho_{sol} - \rho_{gas})^n \qquad (6)$$

where γ_{sol} is the interfacial tension of the solution, P is the parachor, ρ_{sol} is the density of the polymer and ρ_{gas} is the density of the gas and n is the Macleod's exponent. The exponent n is close to 4 for many unassociated liquids of low-molecular-weight substances [51]. In our case, interfacial tension data collapse on a single curve, as reported in Fig. 9. The parachor is, in our case, equal to 3.156 while Macleod's exponent is equal to 3.33.

Fig. 8. Effect of temperature (a) and gas pressure (b) on the interfacial tension; 80 °C (●); 90 °C (△); 100 °C (♦).

Fig. 10. Comparison of the proposed fully experimental approach (full symbols) with the semi-empirical one (open symbols): (a) specific volume of the polymer–gas solution as a function of gas pressure; (b) interfacial tension of the solution as function of gas concentration. Data refer to 90 °C.

The values of the interfacial tension of the solution can be also correlated to CO_2 concentration by using the following empirical equation [52]

$$\gamma_{sol} = (1 - \omega_{ACT})\gamma_{pol}^{1/r} \tag{7}$$

where γ_{sol} is the interfacial tension of the solution, ω_{ACT} is the weight fraction of the dissolved fluid. From the fitting of the experimental data in the whole temperature range (not shown), the parameter r was estimated to be equal to 0.222.

Finally, it is useful to compare the properties obtained according this fully experimental technique with those obtained by a semi-empirical approach. In particular, Fig. 10a reports the values of specific volume of the polymer–gas solution as calculated as by the procedure adopted in the present contribution and those calculated by using the SL-EoS semi-empirical approach, as described in Section 3.1. Furthermore, the comparison has been performed also in terms of interfacial tension, as shown in Fig. 10b. In particular, the semi-empirical interfacial tension data have been derived by using the predicted values of polymer–gas solution specific volume into the fitting of the experimental drops. These comparisons highlight the differences among the fully experimental based calculations and the properties derived on the basis of theoretical assumptions, thus evidencing the importance of the adopted coupled measurement to obtain a reliable estimation of the solution properties.

4. Conclusions

Simultaneous measurement of solubility, diffusivity, specific volume and interfacial tension of molten PCL/CO_2 solutions has been performed at three different temperatures and at CO_2 pressures up to 4.2 MPa. Solubility, as expected, increased with CO_2 pressure and decreased with temperature; data were modeled by using Sanchez–Lacombe theory and the interaction parameter, ψ, in the whole pressure and temperature range, was equal to 0.976 ± 0.001. Mutual diffusivity coefficients have been found to have no significant dependence on CO_2 concentration in the range of investigated pressure and temperature and they increased with temperature with an Arrhenius-type dependence. Quite interestingly, specific volume of the PCL/CO_2 solution was found to show a non monotonic profile, that has been justified hypothesizing that CO_2 within molten PCL is present in two forms: species "associated" and species "nonassociated" with PCL. Associated ones prevail at low pressure, thus being responsible for a volume of mixing smaller than that calculated on the basis of simple volume additivity. Interfacial tension of the solution was found to decrease, with a nearly linear trend, with gas concentration and temperature. Macleod empirical approach provided the description of the relationship between the interfacial tension and the density differences of the two phases in equilibrium (gas and polymer/gas solution), with a collapse of the whole set of data at the different temperatures on a single master curve.

Acknowledgments

References

[1] D.L. Tomasko, H. Li, X. Han, J.M. Wingert, J.L. Lee, A review of CO_2 applications in the processing of polymers, Industrial & Engineering Chemistry Research 42 (2003) 6431–6456.

[2] D.J. Mooney, D.F. Baldwin, N.P. Suh, J.P. Vacanti, R. Langer, Novel approach to fabricate porous sponges of poly(D,L-lactic-co-glycolic acid) without the use of organic solvents, Biomaterials 17 (1996) 1417–1422.

[3] L.J.M. Jacobs, M.F. Kemmere, J.T.F. Keurentjes, Sustainable polymer foaming using high pressure carbon dioxide: a review on fundamentals, processes and applications, Green Chemistry 10 (2008) 731–738.

[4] D.F. Baldwin, C.B. Park, N.P. Suh, A microcellular processing study of poly(ethylene terephthalate) in the amorphous and semicrystalline states. Part I: Microcell nucleation, Polymer Engineering & Science 36 (1996) 1437–1445.

[5] E. Di Maio, G. Mensitieri, S. Iannace, L. Nicolais, W. Li, R.W. Flumerfelt, Structure optimization of polycaprolactone foams by using mixtures of CO_2 and N_2 as blowing agents, Polymer Engineering & Science 45 (2005) 432–441.

[6] C. Marrazzo, E. Di Maio, S. Iannace, L. Nicolais, Process–structure relationships in PCL foaming, Journal of Cellular Plastics 44 (2008) 37–52.

[7] C.B. Park, D.F. Baldwin, N.P. Suh, Effect of the pressure drop rate on the cell nucleation in continuous processing of microcellular polymers, Polymer Engineering & Science 35 (1995) 432–440.

[8] M.A. Shafi, R.W. Flumerfelt, Initial bubble growth in polymer foam processes, Chemical Engineering Science 52 (1997) 627–633.

[9] K. Taki, Experimental and numerical studies on the effects of pressure release rate on number density of bubbles and bubble growth in a polymeric foaming process, Chemical Engineering Science 63 (2008) 3643–3653.

[10] Y.B. Zeldovich, On the theory of new phase formation, cavitation, Acta Physicochimica URSS 18 (1943) 1–12.

[11] J.S. Colton, N.P. Suh, Nucleation of microcellular foam: theory and practice, Polymer Engineering & Science 27 (1987) 500–503.

[12] S.K. Goel, E.J. Beckman, Generation of microcellular polymeric foams using supercritical carbon dioxide. I: Effect of pressure and temperature on nucleation, Polymer Engineering & Science 34 (1994) 1137–1147.

[13] J.H. Han, C.D. Han, Bubble nucleation in polymeric liquids. I. Bubble nucleation in concentrated polymer solutions, Journal of Polymer Science, Part B: Polymer Physics 28 (1990) 711–741.

[14] Y.-M. Corre, A. Maazouz, J. Duchet, J. Reignier, Batch foaming of chain extended PLA with supercritical CO_2: influence of the rheological properties and the process parameters on the cellular structure, Journal of Supercritical Fluids 58 (2011) 177–188.

[15] R. Liao, W. Yu, C. Zhou, Rheological control in foaming polymeric materials: II. Semi-crystalline polymers, Polymer 51 (2010) 6334–6345.

[16] Y. Di, S. Iannace, E. Di Maio, L. Nicolais, Reactively modified poly (lactic acid): properties and foam processing, Macromolecular Materials and Engineering 290 (2005) 1083–1090.

[17] E. Di Maio, S. Iannace, G. Mensitieri, L. Nicolais, A predictive approach based on the Simha–Somcynsky free-volume theory for the effect of dissolved gas on viscosity and glass transition temperature of polymeric mixtures, Journal of Polymer Science, Part B: Polymer Physics 44 (2006) 1863–1873.

[18] C. Marrazzo, E. Di Maio, S. Iannace, Conventional and nanometric nucleating agents in poly(ε-caprolactone) foaming: crystals vs. bubbles nucleation, Polymer Engineering & Science 48 (2008) 336–344.

[19] L. Sorrentino, E. Di Maio, S. Iannace, Poly(ethylene terephthalate) foams: correlation between the polymer properties and the foaming process, Journal of Applied Polymer Science 116 (2010) 27–35.

[20] J.G. Lee, R.W. Flumerfelt, A refined approach to bubble nucleation and polymer foaming process: dissolved gas and cluster size effects, Journal of Colloid and Interface Science 184 (1996) 335–348.

[21] J.M. Andreas, E.A. Hauser, W.B. Tucker, Boundary tension by pendant drops, Journal of Physical Chemistry 42 (1938) 1001–1019.

[22] T. Young, An essay on the cohesion of fluids, Philosophical Transactions of the Royal Society of London 95 (1805) 65–87.

[23] P.S. Laplace, Traitè de Mécanique Céleste, Supplement to Book 10, Gauthier-Villars, Paris, 1805, pp. 771–777.

[24] S. Bashforth, J.C. Adams, An Attempt to Test Capillary Action, Cambridge University Press/Deighton, Bell and Co., London, 1882, pp. 13–56.

[25] O.I. del Rio, A.W. Neumann, Axisymmetric drop shape analysis: computational methods for the measurement of interfacial properties from the shape and dimensions of pendant and sessile drops, Journal of Colloid and Interface Science 196 (1997) 136–147.

[26] P. Cheng, D. Li, L. Boruvka, Y. Rotenberg, A.W. Neumann, Automation of axisymmetric drop shape analysis for measurements of interfacial tensions and contact angles, Colloids and Surfaces 43 (1990) 151–167.

[27] G. Li, J. Wang, C.B. Park, R. Simha, Measurement of gas solubility in linear/branched PP melts, Journal of Polymer Science, Part B: Polymer Physics 45 (2007) 2497–2508.

[28] R.G. Wissinger, M.E. Paulaitis, Molecular thermodynamic model for sorption and swelling in glassy polymer–CO_2 systems at elevated pressures, Industrial & Engineering Chemistry Research 30 (1991) 842–851.

[29] R.G. Wissinger, M.E. Paulatis, Swelling and sorption in polymer–CO_2 mixtures at elevated pressures, Journal of Polymer Science, Part B: Polymer Physics 25 (1987) 2497–2510.

[30] N.M.B. Flichy, S.G. Kazarian, C.J. Lawrence, B.J. Briscoe, An ATR-IR study of poly (dimethylsiloxane) under high-pressure carbon dioxide: simultaneous

measurement of sorption and swelling, Journal of Physical Chemistry B 106 (2002) 754–759.

[31] I.C. Sanchez, R.H. Lacombe, An elementary molecular theory of classical fluids. Pure fluids, Journal of Physical Chemistry 80 (1976) 2352–2362.

[32] I.C. Sanchez, R.H. Lacombe, Elementary equation of state for polymer liquids, Journal of Polymer Science, Part B: Polymer Letters Edition 15 (1977) 71–75.

[33] I.C. Sanchez, R.H. Lacombe, Statistical thermodynamics of polymer solutions, Macromolecules 11 (1978) 1145–1156.

[34] R. Simha, T. Somcynsky, On the statistical thermodynamics of spherical and chain molecule fluids, Macromolecules 2 (1969) 342–350.

[35] G. Li, J. Wang, C.B. Park, Investigating the solubility of CO_2 in polypropylene using various EOS models, Cellular Polymers 25 (2006) 237–248.

[36] Ph.T. Jaeger, J.v. Schnitzler, R. Eggers, Interfacial tension of fluid systems considering the nonstationary case with respect to mass transfer, Chemical Engineering & Technology 19 (1996) 197–202.

[37] K. Dimitrov, L. Boyadzhev, R. Tufen, Properties of supercritical CO_2 saturated poly(ethyleneglycol)nonylphenylether, Macromolecular Chemistry and Physics 200 (1999) 1626–1629.

[38] H. Park, C.B. Park, C. Tzoganakis, K.-H. Tan, P. Chen, Simultaneous determination of the surface tension and density of polystyrene in supercritical nitrogen, Industrial & Engineering Chemistry Research 47 (2008) 4369–4373.

[39] M.G. Pastore Carbone, E. Di Maio, E. Iannace, G. Mensitieri, Simultaneous experimental evaluation of solubility, diffusivity, interfacial tension and specific volume of polymer/gas solutions, Polymer Testing 30 (2011) 303–309.

[40] R.T. Dehoff, Thermodynamics in Materials Science, McGraw-Hill, New York, 1993, pp. 409–464.

[41] J. Crank, The Mathematics of Diffusion, 2nd ed., Oxford University Press, Oxford, 1975, pp. 47–64.

[42] J.S. Vrentas, J.L. Duda, Analysis of step-change sorption experiments, Journal of Polymer Science: Polymer Physics Edition 15 (1977) 2039–2045.

[43] I.C. Sanchez, R.H. Lacombe, Statistical thermodynamics of fluid mixtures, Journal of Physical Chemistry 80 (1976) 2568–2580.

[44] S. Cotugno, E. Di Maio, C. Ciardiello, S. Iannace, G. Mensitieri, L. Nicolais, Sorption thermodynamics and mutual diffusivity of carbon dioxide in molten polycaprolactone, Industrial & Engineering Chemistry Research 42 (2003) 4398–4405.

[45] M.B. Kiszka, M.A. Meilchen, M.A. McHugh, Modeling high-pressure gas–polymer mixtures using the Sanchez–Lacombe equation of state, Journal of Applied Polymer Science 36 (1998) 583–597.

[46] S.P. Nalawade, F. Picchioni, L.P.B.M. Janssen, D.W. Grijpma, J. Feijen, Investigation of the interaction of CO_2 with poly (L-lactide), poly(DL-lactide) and poly(ε-caprolactone) using FTIR spectroscopy, Journal of Applied Polymer Science 109 (2008) 3376–3381.

[47] D. Liu, D.L. Tomasko, Carbon dioxide sorption and dilation of poly(lactide-co-glycolide), Journal of Supercritical Fluids 39 (2007) 416–425.

[48] H. Li, L.J. Lee, D.L. Tomasko, Effect of carbon dioxide on the interfacial tension of polymer melts, Industrial & Engineering Chemistry Research 43 (2004) 509–514.

[49] K.L. Harrison, S.R.P. da Rocha, M.Z. Yates, K.P. Johnston, D. Canelas, J.M. De Simone, Interfacial activity of polymeric surfactants at the polystyrene–carbon dioxide interface, Langmuir 14 (1998) 6855–6863.

[50] K.L. Harrison, K.P. Johnston, I.C. Sanchez, Effect of surfactants on the interfacial tension between supercritical carbon dioxide and polyethylene glycol, Langmuir 12 (1996) 2637–2644.

[51] D.B. Macleod, On a relation between surface tension and density, Transactions of the Faraday Society 19 (1923) 38–41.

[52] R. Reid, J.M. Prausnitz, B.E. Poling, The Properties of Gases and Liquids, 4th ed., McGraw-Hill International Editions, Singapore, 1988, pp. 656–732.